

# Hadean diamonds in zircon from Jack Hills, Western Australia

Martina Menneken<sup>1</sup>, Alexander A. Nemchin<sup>2</sup>, Thorsten Geisler<sup>1</sup>, Robert T. Pidgeon<sup>2</sup> & Simon A. Wilde<sup>2</sup>

Detrital zircons more than 4 billion years old from the Jack Hills metasedimentary belt, Yilgarn craton, Western Australia, are the oldest identified fragments of the Earth's crust<sup>1,2</sup> and are unique in preserving information on the earliest evolution of the Earth. Inclusions of quartz, K-feldspar and monazite in the zircons<sup>3</sup>, in combination with an enrichment of light rare-earth elements<sup>4,5</sup> and an estimated low zircon crystallization temperature<sup>6</sup>, have previously been used as evidence for early recycling of continental crust, leading to the production of granitic melts in the Hadean era. Here we present the discovery of microdiamond inclusions in Jack Hills zircons with an age range from  $3,058 \pm 7$  to  $4,252 \pm 7$  million years. These include the oldest known diamonds found in terrestrial rocks, and introduce a new dimension to the debate on the origin of these zircons and the evolution of the early Earth<sup>6–10</sup>. The spread of ages indicates that either conditions required for diamond formation were repeated several times during early Earth history or that there was significant recycling of ancient diamond. Mineralogical features of the Jack Hills diamonds—such as their occurrence in zircon, their association with graphite and their Raman spectroscopic characteristics—resemble those of diamonds formed during ultrahigh-pressure metamorphism and, unless conditions on the early Earth were unique, imply a relatively thick continental lithosphere and crust–mantle interaction at least 4,250 million years ago.

Research on  $>3,900$ -Myr-old zircon grains from the Jack Hills has mainly focused on their chemical and isotopic compositions. In this study, we have investigated the mineral inclusions in 1,000 randomly chosen zircon grains, collected from a sample of the Jack Hills zircon conglomerate from the initial 'discovery' site<sup>1</sup>. U–Pb ages of the zircon grains were determined using a sensitive high-resolution ion microprobe (SHRIMP II), following the analytical procedure described in detail elsewhere<sup>11,12</sup>. Optical examination revealed that about half of the zircon population contains inclusions larger than  $\sim 1 \mu\text{m}$ . These inclusions were further investigated by confocal micro-Raman spectroscopy. A Raman spectrum of a mineral reflects both its structural and chemical properties and can thus be used as a fingerprint for its identification. We have identified apatite, quartz, xenotime, monazite, rutile, biotite, amphibole, K-feldspar and plagioclase inclusions in the Jack Hills zircon, some of which have also been recognized in previous studies<sup>3,4</sup>. In addition, we unambiguously identified diamond inclusions in 45 zircon grains, mostly associated with graphite, but in some cases with apatite and quartz.

The Raman spectrum of diamond is characterized by a single first-order band near  $1,332 \text{ cm}^{-1}$  with a typical width (full-width at half-maximum, FWHM) of  $\sim 1.7 \text{ cm}^{-1}$ , reflecting a triply degenerate C–C stretching vibration with  $F_{2g}$  symmetry, and sometimes by a second-order feature near  $2,600 \text{ cm}^{-1}$  (ref. 13). The Raman spectra of most of the diamond inclusions ('diamond 1') in the Jack Hills zircons

display the characteristic diamond band at a frequency between  $1,329$  and  $1,332 \text{ cm}^{-1}$  (Fig. 1a). None of the diamonds show a second-order spectral feature near  $2,600 \text{ cm}^{-1}$ . Some inclusions ('diamond 2'), however, show an intense band between  $1,320$  and  $1,327 \text{ cm}^{-1}$  (Fig. 1b) that is further characterized by a larger width compared with that of diamond 1 (Fig. 2). Despite the downshift and broadening, the bands are still symmetric (Fig. 1c, d). At the margin of some diamond inclusions, we obtained spectra that show bands of diamond 1 and 2

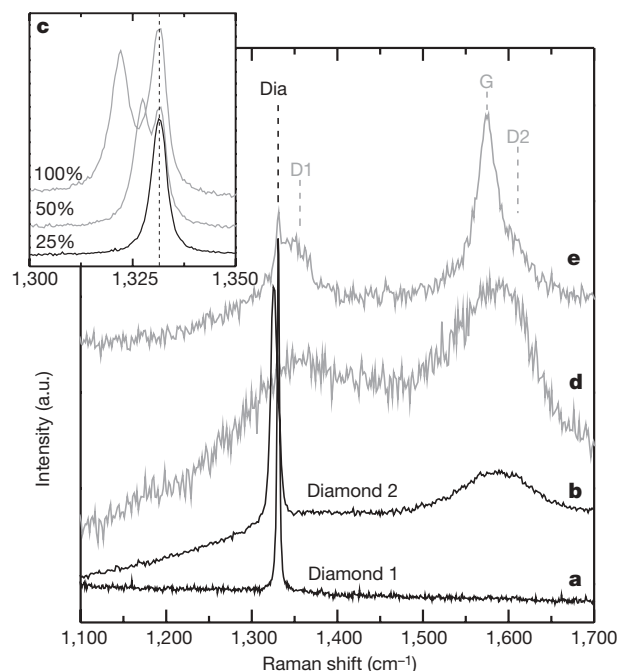


**Figure 1 | Representative Raman spectra of diamond and graphite inclusions in zircon from Jack Hills.** **a**, Raman spectrum showing the first-order Raman band of diamond near  $1,332 \text{ cm}^{-1}$  with a relatively small band width (diamond 1). **b**, Representative spectrum of diamond inclusions that are characterized by a broadened band located between  $1,320$  and  $1,327 \text{ cm}^{-1}$  (diamond 2). **c**, Raman spectra of a diamond inclusion that is characterized by two bands, representing diamond 1 and 2, measured with different laser intensities. The 100% spectrum was measured with full laser power. Note the blue shift of the left band with decreasing laser power, which demonstrates sample heating effects and indicates that diamond 2 is polycrystalline diamond of variable crystallite sizes. **d**, Raman spectrum of graphite with the broad first-order band (G band) near  $1,580 \text{ cm}^{-1}$  and a relative weak disorder band (D1 band) near  $1,350 \text{ cm}^{-1}$  (for a 532 nm excitation). **e**, Spectrum of a diamond–graphite composite inclusion. Note that the graphite bands are sharper than those shown in **c** and that an additional disorder band near  $1,620 \text{ cm}^{-1}$  is visible (D2 band).

<sup>1</sup>Institut für Mineralogie, Westfälische Wilhelms-Universität, Corrensstr. 24, 48149 Münster, Germany. <sup>2</sup>Department of Applied Geology, Western Australian School of Mines, Curtin University of Technology, Bentley, Western Australia 6102, Australia.

overlapping each other. In contrast to the characteristic band of diamond 1, the band of diamond 2 shifts towards higher wavenumbers, when decreasing the laser power (Fig. 1c), indicating heating effects induced in diamond 2 by the incident laser. It has been shown<sup>14</sup> that heating effects in diamond powders of grain sizes down to 0.1  $\mu\text{m}$  can cause a size-dependent frequency shift towards 1,320  $\text{cm}^{-1}$  that is associated with symmetric band broadening, as a result of different thermal properties of microcrystalline diamond. Hence, the band width–frequency relationship of diamond 2, seen in Fig. 2, reflects the occurrence of polycrystalline diamond of variable grain size that is associated with larger diamonds in some inclusions (Fig. 1c).

A major Raman-active vibration near 1,326  $\text{cm}^{-1}$  and an additional band near 1,175  $\text{cm}^{-1}$  (ref. 15), characteristic of lonsdaleite (a hexagonal polytype of diamond, which has been reported from impact structures<sup>16</sup>), were not observed in the present study (Fig. 1). However, we have identified graphite associated with most diamond inclusions by its broad first-order Raman band near 1,580  $\text{cm}^{-1}$  ('G band') and in some cases by its disorder band ('D1 band') near 1,350  $\text{cm}^{-1}$  (for a 532 nm excitation) and its second disorder band ('D2 band') near 1,620  $\text{cm}^{-1}$  (Fig. 1d and e)<sup>17</sup>.

The diamond inclusions have rounded to hexagonal, oval (Fig. 3), angular, or even needle-like shapes. Commonly, graphite is found surrounding diamond, suggesting that it formed after the diamond as a result of retrograde transformation. Diamonds that are exposed at the polished surfaces of the grains can be recognized by their bright cathodoluminescence (CL) intensity, distinguishing them from exposed graphite which gives no CL signal (Figs 3a and d). The secondary electron image in Fig. 3e shows a relatively large, exposed diamond aggregate (giving the spectrum shown in Fig. 1a), which

was originally surrounded by graphite that has now been polished away.

The presence of diamond inclusions in zircon raises the question of whether these diamonds could be the result of contamination from the De Beers diamond polishing powder used in preparing the zircon mounts. However, this can be ruled out as (1) some diamond inclusions are completely enclosed by zircon (Fig. 3b and c), (2) most diamonds reveal variable spectral features that clearly distinguish them from those of the diamond particles in the polishing powder (Fig. 2), (3) the size of the diamond inclusions ranges between 6 and 70  $\mu\text{m}$  so that they are mostly larger than the diamond particles in the polishing materials (<12  $\mu\text{m}$ ), and (4) almost all of the diamonds are associated with graphite (Fig. 1d), which is not present in the polishing powder.

The diamond-bearing zircon crystals are characterized by highly variable internal structures in CL images, typical of the whole Jack Hills population<sup>5,18</sup>. These include simple oscillatory growth zones (Fig. 3d) that are typical of zircon crystals grown from a melt or fluid phase, and irregularly curved growth zones (Fig. 3a) that indicate zircon re-equilibration in an aqueous fluid or melt<sup>19</sup>. Those zones containing diamond show a distribution of <sup>207</sup>Pb/<sup>206</sup>Pb ages similar to the average statistical age distribution of the Jack Hills zircon population<sup>5,20</sup> with a pronounced peak between 3,200 and 3,400 Myr and with ~10% of the population being older than 3,900 Myr (Supplementary Table 1). We found no correlation between the presence of diamond and the age, the internal growth structure, or the Th/U of the host zircon crystals (Supplementary Table 1). Moreover, the polycrystalline microdiamonds (diamond 2) occur in all age groups (Fig. 2). The three oldest diamond-bearing zircon grains gave concordant ages (Myr) of 4,096  $\pm$  4 (1 $\sigma$ ), 4,132  $\pm$  5 (1 $\sigma$ ) and 4,252  $\pm$  7 (1 $\sigma$ ) (Fig. 3d), making them the oldest known diamonds found in terrestrial rocks. The previously known oldest terrestrial diamonds, with a maximum age defined by garnet inclusions at 3,300  $\pm$  200 Myr, are diamonds found in 90-Myr-old kimberlites from Finsch and Kimberley in South Africa<sup>21</sup>.

To evaluate the mode of formation of the Jack Hills diamonds, it is useful to compare the observed mineralogical features with those from diamonds formed under known geological conditions. Natural diamonds form under pressures of >3.2 GPa and temperatures between ~650 and 1,200 °C in the Earth's interior at a depth of >100 km or during meteoritic impact events<sup>22</sup>. Until now, diamonds have been found in (1) primitive carbonaceous chondrites, (2) meteoritic impact structures, (3) kimberlites and lamproites, which delivered them from the subcontinental lithosphere, (4) komatiites, and (5) in crustal rocks, typically sedimentary, that have been subjected to ultrahigh-pressure (UHP) metamorphic conditions<sup>22</sup>.

UHP metamorphic terranes are at present the only known setting where microdiamonds, about 3–50  $\mu\text{m}$  in size, have been reported as inclusions in zircon<sup>23–25</sup>. Also, secondary graphite is commonly associated with diamonds that formed in UHP terranes<sup>26,27</sup> owing to the relatively slow exhumation rates compared to the rate of kimberlite magma ascent, which allows the transformation of diamond to graphite. We further note that the Raman spectral features of diamond 1 agree well with those reported for UHP diamonds<sup>23,25–28</sup>, and are readily distinguished from those of shock-related diamonds and from diamonds found in kimberlites and lamproites (Fig. 2). The latter diamonds are also characterized by a second-order Raman band near 2,600  $\text{cm}^{-1}$  that has not been observed in the present study.

So far we have not detected high-pressure minerals other than diamond in the Jack Hills zircon crystals. There is also no evidence that the observed quartz inclusions were derived from its high-pressure polymorph coesite. The overall mineral inclusion assemblage is essentially granodioritic to granitic (Supplementary Table 1), which resembles the mineral paragenesis commonly associated with carbonados. Carbonados are large polycrystalline nodules that consist of euhedral diamond crystals (typically up to 200  $\mu\text{m}$ )

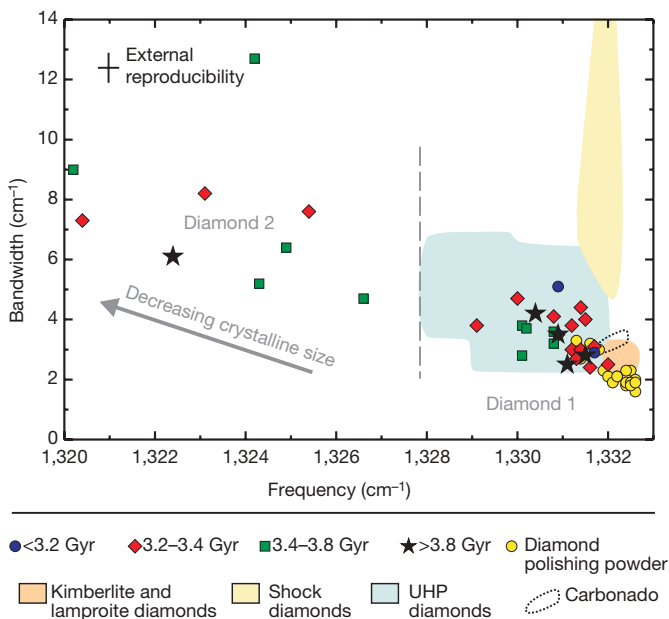


**Figure 2 | Raman data from diamond inclusions in the Jack Hill zircons, from diamond polishing particles, and from diamonds of different geological origin.** Shown is the width (given as FWHM and corrected for instrumental broadening) of the first-order diamond Raman band as a function of frequency for diamond inclusions in zircon crystals from Jack Hills and for diamond polishing particles. The line broadening and frequency red-shift of diamond 2 reflects sample heating effects as a result of variable grain sizes, as marked by the arrow (see Fig. 1). Note that diamonds with different Raman spectral features (diamond 1 and 2) occur within all age groups of the detrital Jack Hills zircon population. Age groups are defined using the corresponding <sup>207</sup>Pb/<sup>206</sup>Pb zircon ages (see Supplementary Table 1). Published Raman data<sup>25,26,28,31</sup> and our own measurements (given in Supplementary Table 2) of diamonds of different origin (shown as coloured fields) are included for comparison.

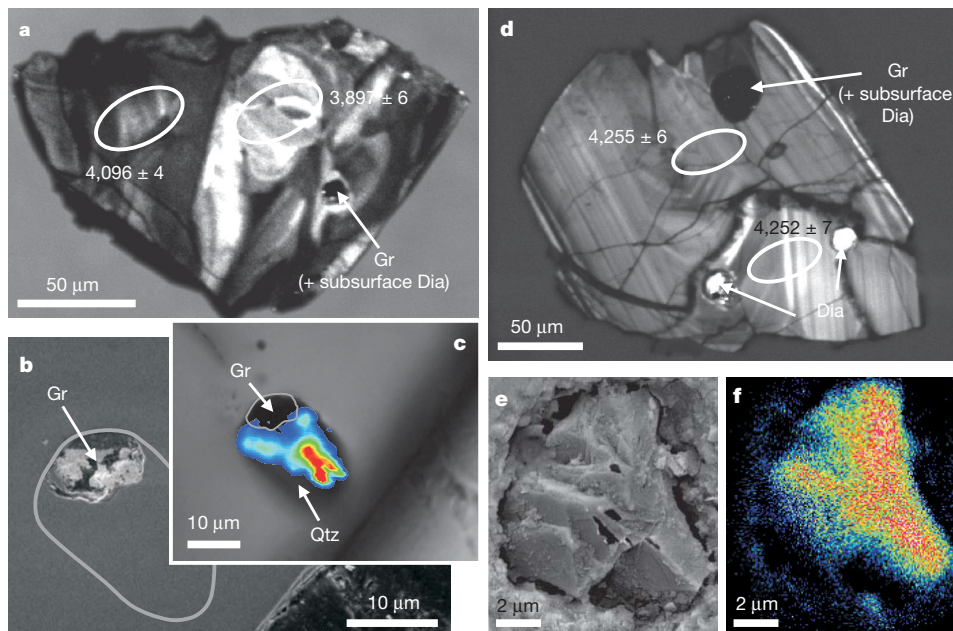


**Figure 3 | Mineralogical features of diamond inclusions in Jack Hills zircon samples. a–c, Grain JH15-142; d–f, grain JH3-20. a, Cathodoluminescence (CL) image of grain JH15-142. Gr, graphite. b, Backscattered electron (BSE) image of the area around the graphite–diamond composite inclusion shown in a. The bright BSE intensity inner region where the inclusion is exposed to the surface is from relict gold coating covering graphite. The dimension of the inclusion, as visible in the transmitted light image shown in c, is outlined by the grey curve. c, Transmitted light image of the same inclusion as shown in Fig. 1b. The part of the inclusion that is exposed to the surface (see b) is outlined by the grey curve. The coloured contours in overlay show the**

intensity distribution of the first-order Raman band of diamond near  $1,332\text{ cm}^{-1}$ . Note that the diamond is included inside the zircon. Qtz, quartz. d, CL image of grain JH3-20. Dia, diamond. e, Secondary electron image of inclusion 20-3, which is visible in the right corner of the zircon grain shown in d. f, Carbon distribution of inclusion 20-3 as obtained by energy-dispersive X-ray analysis. Note that carbon signals at the border of the inclusion result from remnant graphite. White ellipses in a and d mark the SHRIMP analytical sites; numbers show the  $^{207}\text{Pb}/^{206}\text{Pb}$  ages (in Myr) with the  $1\sigma$  uncertainty. Intensity variations in c and f scale from blue (low intensity) to red (high intensity).

set in a matrix of microcrystalline diamond and are associated with crustal minerals such as quartz, orthoclase, xenotime and zircon<sup>29</sup>. Their origin is enigmatic, but theories include metamorphism of earliest subducted lithosphere, radioactive transformation of mantle hydrocarbons, and meteoritic impact on a concentrated biomass<sup>29</sup>. However, the Raman spectral characteristics of carbonados that we have measured are more similar to those of kimberlite- or lamproite-derived diamond rather than to those found in Jack Hills zircon (Fig. 2).

The absence of high-pressure minerals except diamond, together with the occurrence of diamonds in zircons with a range of primary and secondary internal structures (Fig. 3) and the highly variable Th/U ratios (Supplementary Table 1), which do not support formation of zircon at UHP metamorphic conditions, presents a significant problem for the interpretation of the origin of the diamonds and the crystallization history of the zircons. These observations suggest that the diamonds and at least some of their host zircons were formed under different pressure–temperature conditions. It is possible that the diamonds were formed during a single event before or at  $4,252 \pm 7$  Myr ago, which is the crystallization age of the oldest diamond-bearing zircon from the Jack Hills conglomerate (Fig. 3d). This hypothesis may be supported by the Hf-isotope compositions previously determined for Jack Hills zircon<sup>7,30</sup>, which were interpreted to reflect extensive reworking of material separated from the mantle before about 4,140 Myr ago<sup>30</sup>. Diamonds found in younger zircon grains would then be a result of recycling of the older material. Alternatively, diamonds could have been incorporated in zircon at several periods in early Earth history by repetition of the process that resulted in diamond formation.

Many questions remain regarding the origin of the diamonds and their incorporation in the Jack Hills zircons. However, the comparison of the observed mineralogical features of these diamonds with those formed under known geological conditions, particularly their

Raman spectral characteristics and their occurrence with graphite in zircon, indicates that they share more similarities with UHP metamorphic diamonds than with any other known type. If correct, and unless unknown processes operated during the Earth's earliest history, this would imply the presence of a relatively thick continental lithosphere and that crust–mantle interaction occurred on Earth as early as 4,250 Myr ago.

## METHODS SUMMARY

**Raman spectroscopy.** Laser-Raman spectra were collected with a Jobin Yvon HR800 dispersive Raman spectrometer using the 532 nm line of a 14 mW Nd-YAG laser. The scattered Raman light was analysed with a  $100\times$  objective in  $180^\circ$  backscatter geometry and a charged-coupled device (CCD) detector after being dispersed by a grating of 600 grooves  $\text{mm}^{-1}$ . The diamond inclusions were re-measured for quantitative determination of the position and width of the first-order diamond band with a spectral resolution of  $1.1\text{ cm}^{-1}$  (near  $1,330\text{ cm}^{-1}$ ) using a grating of 1,800 grooves  $\text{mm}^{-1}$ .

Raman images of the diamond-graphite-(quartz) composite inclusion (Fig. 3c) as well as measurements of the diamond powder were performed with an ISA LabRam dispersive Raman spectrometer using the 632.187 nm line of a He-Ne laser and a grating of 1,800 grooves  $\text{mm}^{-1}$ , yielding a spectral resolution of  $1.6\text{ cm}^{-1}$ .

**Sensitive high-resolution ion microprobe (SHRIMP).** The filtered ( $\text{O}_2^-$ ) beam with intensity between 2 and 3 nA was focused on the surface of samples into  $\sim 20\text{ }\mu\text{m}$  spot. Secondary ions were passed to the mass spectrometer operating at a mass resolution ( $M/\Delta M$ ) of  $\sim 5,000$ . Each analysis was preceded by a 2 min raster to remove the Au coating. The peak-hopping data collection routine consisted of five scans through the mass stations, with signals measured by an ion counting electron multiplier. Pb/U ratios were calibrated using an empirical correlation between  $\text{Pb}^+/\text{U}^+$  and  $\text{UO}^+/\text{U}^+$  ratios, normalized to the Curtin University standard (a 564-Myr-old Sri Lankan zircon). The 0.8–1.6% error obtained from the multiple analyses of Pb/U ratio on the standard during individual SHRIMP sessions was added in quadrature to the errors observed in the unknowns.

**Full Methods** and any associated references are available in the online version of the paper at [www.nature.com/nature](http://www.nature.com/nature).

**Received 20 April; accepted 6 July 2007.**

- Compston, W. & Pidgeon, R. T. Jack Hills, evidence of more very old detrital zircons in Western Australia. *Nature* **321**, 766–769 (1986).
- Wilde, S. A., Valley, J. W., Peck, W. H. & Graham, C. M. Evidence from detrital zircons for the existence of continental crust and oceans on the Earth 4.4 Gyr ago. *Nature* **409**, 175–178 (2001).
- Maas, R., Kinny, P. D., Williams, I. S., Froude, D. O. & Compston, W. The Earth's oldest known crust: a geochronological and geochemical study of 2900–4200 Ma old zircons from Mt Narryer and Jack Hills, Western Australia. *Geochim. Cosmochim. Acta* **56**, 1281–1300 (1992).
- Peck, W. H., Valley, J. W., Wilde, S. A. & Graham, C. M. Oxygen isotope ratios and rare earth elements in 3.3 to 4.4 Ga zircons: ion microprobe evidence for high  $\delta^{18}\text{O}$  continental crust and oceans in the Early Archaean. *Geochim. Cosmochim. Acta* **65**, 4215–4229 (2001).
- Cavosie, A. J., Valley, J. W. & Wilde, S. A. E. I. M. F. Magmatic  $\delta^{18}\text{O}$  in 4400–3900 Ma detrital zircons: a record of the alteration and recycling of crust in the Early Archaean. *Earth Planet. Sci. Lett.* **235**, 663–681 (2005).
- Watson, E. B. & Harrison, T. M. Zircon thermometer reveals minimum melting conditions on earliest Earth. *Science* **308**, 841–844 (2005).
- Harrison, T. M. *et al.* Heterogeneous Hadean hafnium: Evidence of continental crust at 4.4 to 4.5 Ga. *Science* **310**, 1947–1950 (2005).
- Valley, J. W., Cavosie, A. J., Fu, B., Peck, W. H. & Wilde, S. A. Comment on “Heterogeneous Hadean hafnium: Evidence of continental crust at 4.4 to 4.5 Ga”. *Science* **312**, 1139a (2006).
- Glikson, A. Comment on “Zircon thermometer reveals minimum melting conditions on earliest Earth” I. *Science* **311**, 779a (2006).
- Nutman, A. P. Comment on “Zircon thermometer reveals minimum melting conditions on earliest Earth” II. *Science* **311**, 779b (2006).
- Compston, W., Williams, I. S. & Meyer, C. U-Pb geochronology of zircons from Lunar Breccia 73217 using a sensitive high mass-resolution ion microprobe. *J. Geophys. Res.* **89**, 525–534 (1984).
- Kennedy, A. K. & de Laeter, J. R. The performance characteristics of the WA SHRIMP II ion microprobe. *US Geol. Surv. Circ.* **1107**, 166 (1994).
- Gillet, P., Hemley, R. J. & McMillan, P. F. Vibrational properties of minerals at high pressures and temperatures. *Rev. Min.* **37**, 525–590 (1998).
- Nachal'naya, T. A. & Andreyev, V. D. Shift of the frequency and Stokes-anti-Stokes ratio of Raman spectra from diamond powders. *Diamond Related Mater.* **3**, 1325–1328 (1994).
- Knight, D. S. & White, W. B. Characterization of diamond films by Raman spectroscopy. *J. Mater. Res.* **4**, 385–393 (1989).
- Frondel, C. & Marvin, U. B. Lonsdaleite, a new hexagonal polymorph of diamond. *Nature* **214**, 587–589 (1967).
- Pasteris, J. D. & Wopenka, B. Raman spectra of graphite as indicators of degree of metamorphism. *Can. Mineral.* **29**, 1–9 (1991).
- Nemchin, A. A., Pidgeon, R. T. & Whitehouse, M. J. Re-evaluation of the origin and evolution of >4.2 Ga zircons from the Jack Hills metasedimentary rocks. *Earth Planet. Sci. Lett.* **244**, 218–233 (2006).
- Geisler, T., Schaltegger, U. & Tomaschek, F. Re-equilibration of zircon in aqueous fluids and melts. *Elements* **3**, 45–51 (2007).
- Pidgeon, R. T. & Nemchin, A. A. High abundance of early Archaean grains and the age distribution of detrital zircons in a sillimanite-bearing quartzite from Mt Narryer, Western Australia. *Precamb. Res.* **150**, 201–220 (2006).
- Richardson, S. H., Gurney, J. J., Erlank, A. J. & Harris, J. W. Origin of diamonds in old enriched mantle. *Nature* **310**, 198–202 (1984).
- Haggerty, S. E. A diamond trilogy: superplumes, supercontinents, and supernovae. *Science* **285**, 851–860 (1999).
- De Corte, K. *et al.* Diamond growth during ultrahigh-pressure metamorphism of the Kokchetav Massif, northern Kazakhstan. *Island Arc* **9**, 428–438 (2000).
- Dobrzhinetskaya, L. F. *et al.* Focused ion beam technique and transmission electron microscope studies of microdiamonds from the Saxonian Erzgebirge, Germany. *Earth Planet. Sci. Lett.* **210**, 399–410 (2003).
- Dobrzhinetskaya, L. F. *et al.* Synchrotron infrared and Raman spectroscopy of microdiamonds from Erzgebirge, Germany. *Earth Planet. Sci. Lett.* **248**, 340–349 (2006).
- Perraki, M., Proyer, A., Mposkos, E., Kaindl, R. & Hoinkes, G. Raman micro-spectroscopy on diamond, graphite and other carbon polymorphs from the ultrahigh-pressure metamorphic Kimi Complex of the Rhodope Metamorphic Province, NE Greece. *Earth Planet. Sci. Lett.* **241**, 672–685 (2006).
- Mposkos, E. & Krohe, A. Pressure-temperature-deformation paths of closely associated ultra-high-pressure (diamond-bearing) crustal and mantle rocks of the Kimi complex: implications for the tectonic history of the Rhodope Mountains, Greece. *Can. J. Earth Sci.* **43**, 1755–1776 (2006).
- Korsakov, A. V., Vandenabeele, P. & Theunissen, K. Discrimination of metamorphic diamond populations by Raman spectroscopy (Kokchetav, Kazakhstan). *Spectrochim. Acta A* **61**, 2378–2385 (2005).
- Heaney, P. J., Vicenzi, E. P. & De, S. Strange diamonds: The mysterious origins of carbonado and framesite. *Elements* **1**, 85–89 (2005).
- Amelin, Y., Lee, D.-C., Halliday, A. N. & Pidgeon, R. T. Nature of the Earth's earliest crust from hafnium isotopes in single detrital zircons. *Nature* **399**, 252–255 (1999).
- El Goresy, A. *et al.* In situ discovery of shock-induced graphite-diamond phase transition in gneisses from the Ries Crater, Germany. *Am. Miner.* **86**, 611–621 (2001).

**Supplementary Information** is linked to the online version of the paper at [www.nature.com/nature](http://www.nature.com/nature).

**Acknowledgements** This research was supported by a Curtin University grant to A.A.N. and S. A.W. We further acknowledge the Deutsche Forschungsgemeinschaft for financial support. We also wish to thank E. Scherer, F. Tomaschek and I. Fitzsimons for discussions on earlier versions of the manuscript and J. Schlüter from the Mineralogical Museum of the University of Hamburg and A. Bischoff for providing diamond samples for comparative Raman measurements.

**Author Information** Reprints and permissions information is available at [www.nature.com/reprints](http://www.nature.com/reprints). The authors declare no competing financial interests. Correspondence and requests for materials should be addressed to M.M. ([m\\_menn03@uni-muenster.de](mailto:m_menn03@uni-muenster.de)) or T.G. ([tgeisler@nwz.uni-muenster.de](mailto:tgeisler@nwz.uni-muenster.de)).

## METHODS

**Sample preparation.** Zircon grains (1,000) were hand-picked from a previously prepared  $>135\ \mu\text{m}$  concentrate and mounted onto double-sided adhesive tape, along with pieces of the Curtin University Sri Lankan gem zircon (CZ3) used as standard for the SHRIMP measurements. They were enclosed in epoxy resin disks, ground so as to effectively cut all zircon grains in half, and polished with  $<12\ \mu\text{m}$  De Beers diamond polishing powder.

**Raman spectroscopy.** Laser-Raman spectra of the inclusions were collected with a Jobin Yvon HR800 dispersive Raman spectrometer using the 532 nm line of a Nd-YAG laser with a laser power of 14 mW. The scattered Raman light was analysed with a CCD detector after being dispersed by a grating of 600 grooves  $\text{mm}^{-1}$ . A  $100\times$  objective with a numerical aperture of 0.9 was used on a BX-40 microscope. The diamond inclusions were re-measured with a grating of 1,800 grooves  $\text{mm}^{-1}$  for quantitative determination of the position and width of the first-order diamond band near  $1,332\ \text{cm}^{-1}$ . With the 1,800 grooves  $\text{mm}^{-1}$  grid, the spectral resolution near  $1,332\ \text{cm}^{-1}$  was  $1.1\ \text{cm}^{-1}$ , as measured by neon emission lines. The following equation was used to correct for the effect of the finite slit width on measured band width (given as FWHM)<sup>32</sup>:

$$\Gamma = \Gamma_m [1 - (S/\Gamma_m)^2]$$

where  $\Gamma$ ,  $\Gamma_m$  and  $S$  are the corrected band width of the first-order diamond band, the measured band width, and the spectral slit width, respectively. The frequency was calibrated using the first-order Si line at  $520.7\ \text{cm}^{-1}$  and lines from a neon lamp. The standard errors from the fitting procedure of both the Raman frequency and width were usually less than  $0.2\ \text{cm}^{-1}$ .

We checked for possible heating effects induced by the incident laser power on the Raman spectral features. Larger diamond inclusions (diamond 1) do not show any heating effects as checked by (1) reducing the laser power with filters and (2) measuring the integral intensity of the Stokes and anti-Stokes component in the diamond Raman spectra, which allows the calculation of the local heating temperature<sup>14</sup> (see Fig. 1c). However, some diamonds (diamond 2) show temperature-induced spectral changes, which are used to discriminate between the two types of diamond (see Fig. 1c and Fig. 2).

Raman images of the diamond-graphite-(quartz) composite inclusions as well as measurements of the diamond powder were performed with an ISA LabRam dispersive Raman spectrometer using the 632.187 nm line of a He-Ne laser and a grating of 1,800 grooves  $\text{mm}^{-1}$ . Raman images were obtained after the SHRIMP measurements on re-polished samples. The spectral resolution was  $1.6\ \text{cm}^{-1}$  near  $1,332\ \text{cm}^{-1}$ . The lateral spatial resolution was about  $1\text{--}2\ \mu\text{m}$ . For imaging, a confocal hole of  $500\ \mu\text{m}$  was used.

**Sensitive high-resolution ion microprobe (SHRIMP).** The SHRIMP methodology follows analytical procedure described elsewhere<sup>11,12</sup>. The filtered ( $\text{O}_2^-$ ) beam with intensity between 2 and 3 nA was focused on the surface of samples into an  $\sim 20\ \mu\text{m}$  spot. Secondary ions were passed to the mass spectrometer operating at a mass resolution ( $M/\Delta M$ ) of  $\sim 5,000$ . Each analysis was preceded by a 2 min raster to remove the Au coating. The peak-hopping data collection routine consisted of five scans through the mass stations, with signals measured by an ion counting electron multiplier. Pb/U ratios were calibrated using an empirical correlation between  $\text{Pb}^+/\text{U}^+$  and  $\text{UO}^+/\text{U}^+$  ratios, normalized to the 564-Myr-old Sri Lankan zircon CZ3<sup>33</sup>. The 0.8–1.6% error obtained from the multiple analyses of Pb/U ratio on the standard during individual SHRIMP sessions was added in quadrature to the errors observed in the unknowns. The initial data reduction was done using the SQUID add-in for Microsoft Excel<sup>34</sup>, and Isoplot<sup>35</sup> was applied for further age calculations.

32. Tanabe, K. & Hiraishi, J. Correction of finite slit width effects on Raman line widths. *Spectrochim. Acta A* **36**, 341–344 (1980).
33. Pidgeon, R. T., Furfaro, D., Kennedy, A. K., Nemchin, A. A. & van Bronswijk, W. Calibration of zircon standards for the Curtin SHRIMP. *US Geol. Surv. Circ.* **1107**, 251 (1994).
34. Ludwig, K. *Users Manual for Squid 1.02* (Special Publication 1a, Berkeley Geochronology Center, Berkeley, California, 2001).
35. Ludwig, K. *Users manual for Isoplot/Ex rev. 2.49* (Special Publication 2, Berkeley Geochronology Center, Berkeley, California, 2001).